

Anita Reimer · Olaf Reimer · Martin Pohl

Gamma rays from colliding winds of massive stars

Received: date / Accepted: date

Abstract Colliding winds of massive binaries have long been considered as potential sites of non-thermal high-energy photon production. This is motivated by the detection of non-thermal spectra in the radio band, as well as by correlation studies of yet unidentified EGRET γ -ray sources with source populations appearing in star formation regions.

This work re-considers the basic radiative processes and its properties that lead to high energy photon production in long-period massive star systems. We show that Klein-Nishina effects as well as the anisotropic nature of the inverse Compton scattering, the dominating leptonic emission process, likely yield spectral and variability signatures in the γ -ray domain at or above the sensitivity of current or upcoming gamma ray instruments like GLAST-LAT. In addition to all relevant radiative losses, we include propagation (such as convection in the stellar wind) as well as photon absorption effects, which a priori can not be neglected.

The calculations are applied to WR 140 and WR 147, and predictions for their detectability in the γ -ray regime are provided. Physically similar specimen of their kind like WR 146, WR 137, WR 138, WR 112 and WR 125 may be regarded as candidate sources at GeV energies for near-future γ -ray experiments.

Finally, we discuss several aspects relevant for eventually identifying this source class as a γ -ray emitting population. Thereby we utilize our findings on the expected radiative behavior of typical colliding wind binaries in the γ -ray regime as well as its expected spatial distribution on the γ -ray sky.

Keywords Stars: early-type · Stars: binaries · Stars: winds, outflows · Gamma rays: theory · Radiation mechanisms: non-thermal

PACS 97.20.Ec · 97.80.-d · 97.10.Me · 95.30.Gv

1 Introduction

By far the most convincing evidence for particle acceleration to relativistic energies mediated by the supersonic (terminal velocity $v_\infty \sim 1000\text{-}5000$ km/s) winds of massive ($\dot{M} \sim 10^{-6}\dots^{-5}M_\odot/\text{yr}$), hot ($T \sim 30000 - 50000\text{K}$) stars comes from the observation of non-thermal radio emission (e.g. [1]). This has been interpreted by synchrotron emission on the basis of the measured spectra (much steeper than the canonical value $\alpha_r \sim +0.6$, $F_\nu \propto \nu^{\alpha_r}$) and high brightness temperatures of $\sim 10^{6-7}\text{K}$, far exceeding $\sim 10^4\text{K}$ expected from free-free emission from a steady-state isothermal radially symmetric wind [2]. Those particles have been suggested to be accelerated either in shocks caused by the instability of radiatively driven winds [3], in the shocked wind collision region of multiple systems or in the termination shock [4]. Triggered by these observations it has been quickly realized that γ -ray emission should be expected as well, either through leptonic processes (inverse Compton scattering (IC) of the copious stellar UV photons (e.g. [5]), relativistic bremsstrahlung (e.g. [6]) or hadronic interactions of co-accelerated ions with the dense wind material (e.g. [7,8])). This has established a plausible physical setting for massive star systems being putative γ -ray emitters. Indeed, positional coincidences of Wolf-Rayet (WR) stars with the population of so far unidentified EGRET sources have been found for 13 WR-binary systems [9, 10, 11]. Recently, the presence of non-thermal radio emission has been linked to the binarity status of the stellar systems [12], which supports the picture of particles being predominantly accelerated at the forward and reverse shocks from the colliding supersonic winds from massive stars.

A. & O. Reimer
W.W. Hansen Experimental Physics Laboratory, Stanford University, 445 Via Palou, Stanford, CA 94305, USA
E-mail: afr@stanford.edu, olr@stanford.edu

M. Pohl
Department of Physics and Astronomy, Iowa State University, Ames, Iowa 50011, USA
E-mail: mkp@iastate.edu

In this work we consider long-period binary systems as the most prospective γ -ray emitters detectable by the near-future experiment GLAST-LAT, and extend previous theoretical work by including propagation, and anisotropy and Klein-Nishina (KN) effects of the inverse Compton (IC) scattering process.

2 The broadband SED of colliding wind systems of massive stars

At present, the observationally established broadband spectral energy distribution (SED) of colliding wind binaries (CWBs) ranges from radio wavelengths to X-ray energies. At GHz frequencies, only one third of all observed WRs has been detected (e.g. [13,14]). Roughly 40% of these show signatures of a contributing non-thermal component. These are predominantly binaries with periods > 1 year, and this can be understood as an absorption effect: The winds of massive stars are partially optically thick at radio wavelengths. For typical O-star wind parameters the $\tau_\nu = 1$ surface lies roughly at $\sim (1-2) \times 10^3 R_\odot$ at GHz frequencies. For WR stars these radii are even larger. Thus optically thin sight lines can only be found in systems with stellar separations of $\ll 10^{3-4} R_\odot$. At IR wavelengths, massive binaries often show components in excess to the expected free-free emission (e.g. [15]). These persistent or variable/periodically/episodically appearing IR excess fluxes have been interpreted as signatures of dust formation. The photospheric continuum emission dominates a broad range at optical to UV energies. Excess emission has also been observed at X-ray energies. Some systems show X-ray luminosities up to two orders of magnitude above the values suggested by the canonical relation $L_X/L_{\text{bol}} \sim 10^{-7}$ obeyed by single early-type stars (e.g. [16]). This excess emission has been attributed to the shock-heated ($T \sim 10^7-8\text{K}$) plasma produced in the winds collision region. Indeed, recent Chandra observations of the close-by WR 147 system show extended emission peaking at a location which is in agreement with the expected wind collision region [17]. The observed phase-locked orbital variability in massive binaries in the soft X-ray as well as radio band is mainly a result of absorption in the dense stellar winds along the changing line of sight.

In the following we shall concentrate on the non-thermal part of the continuum emission from CWBs.

3 The model

Various works have been devoted in the past to non-thermal emission components from CWBs (e.g. [5,7,18,19,20], see also references in [21]) based on either leptonic (mostly IC) and/or hadronic (π^0 -decay γ -rays) processes. They generally conclude on γ -ray luminosities in the range $10^{32...35} \text{erg/s}$ to be expected from WR-binaries.

Since the IC process has been shown to likely dominate the γ -ray production (e.g. [19,22]), this process is prone to determine the spectral appearance of WR-binaries at high energies. Here Klein-Nishina as well as anisotropy effects, neglected in past modeling of these systems, may provide valuable features that can be instrumental in identifying this source population at γ -ray energies. Further spectral imprints are expected from particle propagation within the extended colliding wind region. A simplified geometry of the system proves sufficient to highlight these effects.

In the following we consider the sketch of a colliding wind region (CWR) that has been presented by e.g. Eichler & Usov (1993) [19] with the stagnation point defined by balancing the wind momenta with the assumption of spherical homogenous winds. Since in general $M_{WR} > M_{OB}$ and $v_{\infty,WR} \approx v_{\infty,OB}$ the shock distance to the OB-star, x_{OB} , is much smaller than to the WR-star. We shall neglect here the interaction of the stellar radiation fields on the wind structure ([23,24]): This effect is inherent to short-period binaries, and may influence the wind speed, thereby weakening the ram balance, shock strength and temperature. Thus our theoretical considerations here shall be restricted to long-period binaries. The stellar winds are permeated by magnetic fields originating from the surface of the massive star. Estimates for surface magnetic field strengths range from below $B_s = 100 \text{ G}$ (e.g. [25]) up to $\sim 10^4 \text{ G}$ in WR-stars [26]. In the following we fix this value to a reasonable 100 G, unless stated otherwise, and use the well-developed magnetic rotator theory (e.g. [27]) to estimate the field strength B_G (in Gauss) at the CWR. Typically $> \text{mG}$ or higher field strengths are expected, assumed to be constant throughout the emission region, at the CWR in long-period binaries. The shocked high-speed winds are creating a region of hot gas that is separated by a contact discontinuity, and a forward and reverse shock follows. The gas flow velocity in this region away from the stagnation point will be some fraction of the wind velocity which we keep constant at V for simplicity. A simplification of the geometry from a bow-shaped to a cylinder-shaped collision region (with radius r perpendicular to the line-of-centres of the two stars, and given thickness) allows us to solve the relevant continuity equations analytically (see [28]). Here we consider diffusive shock acceleration (with acceleration rate a) out of a pool of thermal particles, and take into account (continuous) radiative losses (synchrotron, IC, bremsstrahlung and Coulomb losses), (energy-independent) diffusion by introducing an escape time T_0 and convection with speed V (set to $V = 1/2v_{OB}$ if not noted otherwise). The maximum particle energy is thereby determined self-consistently.

At a distance $> r_0$ from the stagnation point convection along the post-shock flow will dominate over diffusion. At r_0 diffusion balances convection. Correspondingly, the emission region is divided into a region where acceleration/diffusion dominates, the "acceleration zone",

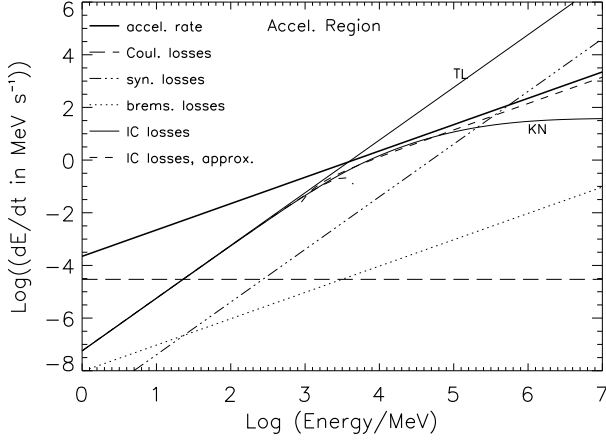


Fig. 1 Energy loss rates in the acceleration zone due to IC scattering (thin solid lines) in the Thomson regime (TL) and KN regime (KN), synchrotron radiation (dashed-triple-dotted line), relativistic electron-ion bremsstrahlung (dashed-dotted line) and Coulomb interactions (dashed line) in comparison to the acceleration rate (thick solid line). Parameters are: bolometric OB-star luminosity $L_{\text{bol,OB}} = 10^5 L_{\odot}$, target photon energy $\epsilon_T = 10$ eV, OB-star mass loss rate $\dot{M}_{\text{OB}} = 10^{-6} M_{\odot} \text{yr}^{-1}$, WR-star mass loss rate $\dot{M}_{\text{WR}} = 10 \dot{M}_{\text{OB}}$, OB-star terminal velocity $v_{\infty, \text{OB}} = 4000 \text{ km/s}$, binary separation $D = 10^{14} \text{ cm}$, $x_{\text{OB}} \approx 0.24D$, surface magnetic field $B_s = 100 \text{ G}$, field strength at the CWR $B \approx 0.5 \text{ G}$, diffusion coefficient $\kappa_a = 1.6 \cdot 10^{20} \text{ cm}^2 \text{ s}^{-1}$, escape time $T_0 \approx 1127$ s, size of the acceleration region $r_0 \approx 8.5 \cdot 10^{11} \text{ cm}$. See [28] for details.

and the outer region where convection dominates, the "convection zone". The steady-state diffusion-loss equation can be solved analytically provided suitable approximations for the KN cross section are applied (see [28]). Fig. 1 shows an example of all loss time scales for typical parameters of WR-binaries. The transition region, between the Thomson and extreme KN range of the IC cross section, appears relevant for typical long-period WR-systems. A rigorous treatment of the Compton losses must therefore include KN effects.

We find electron spectra with smooth roll-overs that cutoff at higher energies as compared to electron spectra that remain in the Thomson approximation throughout the whole particle energy range. In the convection region the particles lose energy radiatively as well as through expansion losses while in the post-shock flow. This leads to a dilution of the particle density as well as a deficit of high energy particles. The corresponding volume-integrated photon spectra softens (see Fig. 2), depending on the relative size of the convection region with respect to the acceleration region. This itself depends on the diffusion and convection time scales operating in the CWR.

With typically the photon to magnetic field energy density $u_{\text{ph}}/u_B \approx 52 L_{\text{bol,OB},\odot} / (B_G x_{\text{OB},\odot})^2 \geq 1$ (where $L_{\text{bol,OB},\odot}$ and $x_{\text{OB},\odot}$ are in units solar luminosity and ra-

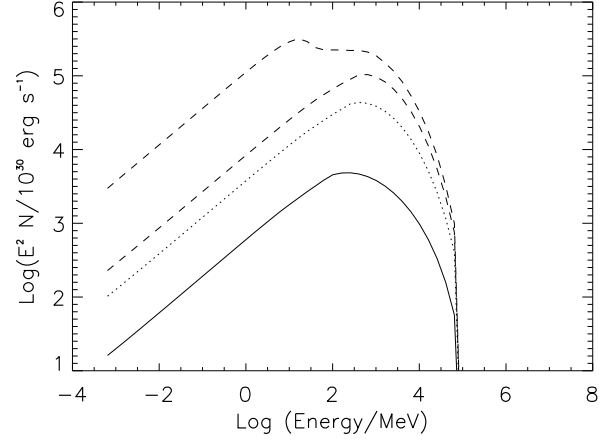


Fig. 2 IC spectra from the acceleration region for $D = 10^{14} \text{ cm}$ and $\theta_L = 0^\circ$ (lower solid line), 30° (lower dashed line), 60° (dotted line), 90° (dashed-dotted line), 120° (dashed-triple dotted line) 150° (long dashed line) and 180° (upper solid line). For $\theta_L = 30^\circ$ the total volume-integrated (i.e. acceleration plus convection zone) IC spectrum is also shown (upper dashed line). All other parameters are the same as in Fig. 1.

dius, respectively) IC scattering turns out to be the most important radiative loss channel for relativistic electrons in CWBs in most cases [19, 22]. Because the stellar target photons for IC scattering arrive at the collision region from a preferred direction, the full angular dependence of the cross section has to be taken into account (e.g. [29]). This leads to anisotropy effects like the emitted flux and cutoff energy being dependent on the sight line into the wind (see Fig. 2). The calculations are carried out using the monochromatic approximation for the photospheric target field and an isotropic particle distribution in the emission region. The latter is maintained by pitch angle scattering at magnetic field inhomogeneities. Fig. 2 shows the maximum flux level reached at phases where the WR-star is behind the OB-star along the sight line. Furthermore, large scattering angles tend to produce more energetic photons than low angles. This can affect the cutoff photon energy by several orders of magnitude for a given value of the electron energy cutoff (see Sect. 4.2).

Details are described in [28].

4 Application to archetypal systems

4.1 WR 140

The archetypal WR-binary system WR 140 (WC 7pd + O4-5 V), located in the Cygnus constellation at a distance of ~ 1.85 kpc, is one of the most detailed studied specimen of its kind. Its long (~ 8 years) period and extreme eccentricity ($e \approx 0.88$) makes it a diverse system

to study its non-thermal behavior in the radio band. For the first time, Dougherty et al. (2005) [30] resolved the bow-shaped arcs of the emission region at 8 epochs of 8.4 GHz VLBA observations. We used the synchrotron spectra and system parameters as published in [30] to predict its non-thermal high energy emission at various phases. With these values the CWR is located at a distance x_{OB} of 0.32 times the stellar separation. For a surface magnetic field of 100 G roughly equipartition values for its field strength at the CWR location follow. With a relativistic particle injection energy of $\sim 10^{-2}\dots-3\%$ of the kinetic wind energy, the synchrotron fluxes at the considered phases (0.2, 0.67, 0.8, 0.95) could be reproduced. From radio observational grounds, relativistic electrons at least up to ~ 10 -100 MeV do exist. This limits the diffusion coefficient κ to sufficiently low values which will allow the acceleration rate to overcome the Coulomb loss rate at low energies. A further constraint of the diffusion coefficient is provided by the spectral shape of the non-thermal radio component, if the shock compression ratio and convection velocity are known. On the other side, κ is limited by Bohm diffusion. For $\kappa = 2 \cdot 10^{19} \text{cm}^2 \text{s}^{-1}$ up to $\sim 10^5 \text{MeV}$ -electrons are expected at least at apastron, where radiative losses are sufficiently small not to affect the cutoff particle energy (see Fig. 3). The self-consistent determination of the maximum particle energy allows sound predictions at the highest energies. Note that KN effects will alter the emitting electron spectrum above $\sim 10^4 \text{MeV}$, as indicated in Fig. 3. This is in contrast to phases close to periastron. The intense stellar radiation field there limits the electron spectrum to $\sim 100 \text{MeV}$ (see Fig. 3). As a consequence, the corresponding photon spectrum from IC scattering cuts off already in the soft γ -ray band (see Fig. 4), and hadronically produced photons may dominate at (sub-)GeV energies, albeit with a possibly undetectable flux level even for the more sensitive near-future experiments. EGRET observations, that were carried out rather around periastron, therefore did not lead to detections. Mainly as a result of including also hadronic ion-ion interactions into the calculations for π^0 production, the corresponding π^0 -decay γ -ray flux in Pittard & Dougherty [31] extends to higher energies than considered here. The association of WR 140 to the unidentified EGRET source 3EG J2022+4317 appears to be vague: With WR 140 being located $\sim 0.67^\circ$ away from the nominal position of 3EG J2022+4317, and barely consistent with the 99% source location uncertainty contour a conclusive identification seems farfetched. It is due to the extreme eccentricity of this system, leading to significant changes in the stellar radiation field density at the shock location, that causes a blurring of the phase-locked flux variations expected otherwise from the anisotropy of the dominating IC scattering process. Indeed, orbital flux variations in this system are reduced to a factor $\sim 2 - 3$ (see Fig. 4). In general, relativistic bremsstrahlung radiation lies always below the IC emission level in these systems. When compared to the ex-

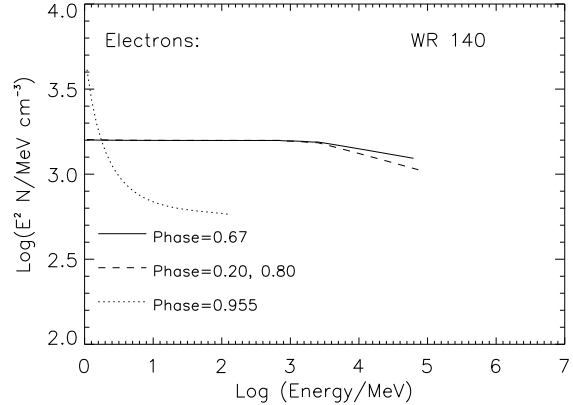


Fig. 3 Steady-state electron spectra for WR 140 at orbital phases 0.955, 0.2, 0.671 and 0.8. Flux is in arbitrary units. See text for parameters.

pected IC flux, π^0 -decay γ -ray production is small, even if the total wind energy is transformed into relativistic protons/ions. This makes WR-binary systems rather unpromising putative neutrino and cosmic ray sources within our model.

Fig. 4 implies that WR 140 may be detectable with GeV-instruments like GLAST-LAT even at individually selected phases if the electrons reach sufficient high energies, while INTEGRAL requires Msec exposures for any detection above 1 MeV. The expected extent of the photon spectrum to $\sim 10 - 100$ GeV at phases where the binary separation is large, may even allow low-energy threshold Imaging Atmospheric Cherenkov Telescopes (IACTs) to gain important information on the cutoff of WR 140's spectrum. This may allow to further constrain the diffusion coefficient. Note that photon absorption due to $\gamma\gamma$ pair production can not a priori be neglected in colliding wind systems. E.g. for WR 140 the optical depth $\tau_{\gamma\gamma}(r = r_0, E \approx 100 \text{GeV}) \sim 1$ at phase 0.67, $\tau_{\gamma\gamma}(r = r_0, E \approx 100 \text{GeV}) \sim 3$ at phase 0.95.

4.2 WR 147

Due to its proximity WR 147 (WN8h + B0.5V) is one of the few binary systems where high resolution radio observations lead to resolving this system into its components (Williams et al. 1997). The observed radio morphology supports a binary separation of ~ 417 AU for a source distance of 650 pc. We used the system parameters as published in Setia Gunawan et al. (2001) [32] together with the observed synchrotron spectrum to model its expected spectral behaviour at high energies. Since WR 147's inclination i nor eccentricity e are known, we assumed for our modeling $e = 0$ and $i = 90^\circ$. The observed synchrotron spectrum could be reproduced within its observational uncertainties if $\sim 0.15\%$ of the OB-wind kinetic energy is transformed into relativistic electrons,

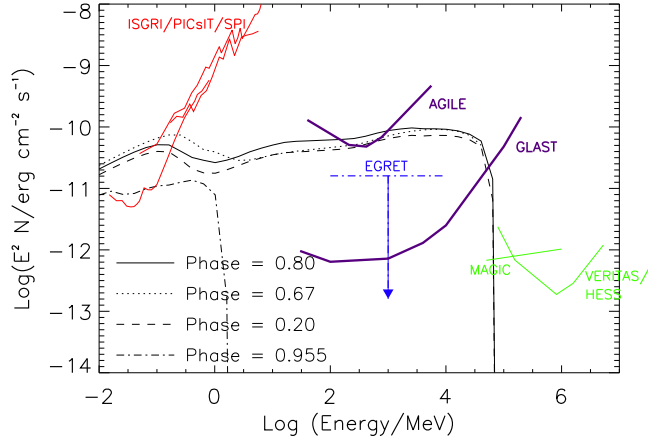


Fig. 4 IC spectra for WR 140 at phases 0.955, 0.2, 0.671 and 0.8 from electron spectra as shown in Fig.3. The spectral changes from γ -ray absorption are not shown here. The EGRET 2σ upper limit [22] is based on observations that correspond to a superposition of orbital states rather determined by periastron phase, and therefore applies rather to phase 0.955.

and assuming a surface magnetic field of 30 G (translating into 25 mG fields at the CWR). Due to its huge binary separation the emitting particle spectra are not limited by IC losses but rather by the size of the acceleration region. Fig. 5 presents the expected orbital IC flux variations due to the anisotropic nature of the IC process for the above described parameter set. Here the maximum flux and photon cutoff energy, expected when the WR-star is behind the OB-star along the sight line, are more than one order of magnitude higher than their minimum values. Absorption of > 50 GeV photons turns out negligible for this system, provided its eccentricity is small. The chance to detect WR 147 with future high sensitive instruments is somewhat better than for WR 140. While LAT will probe the MeV-GeV range of its spectrum, only the low threshold (< 100 GeV) experiments in the northern hemisphere among the ground-based IACTs may have a distinct chance to detect WR 147 at its highest energies.

4.3 Further candidates ?

Our work provides ample evidence for the archetypal long-period WR-binaries WR 140 and WR 147 being plausible candidates for detection with near future γ -ray instruments. Both provide target photon fields at the CWR which is sufficiently dense to produce a IC scattered photon flux above the respective instrument sensitivity, but at the same time does not act as a thick absorber for those photons, nor prevents electron acceleration to high enough energies by radiative losses. A sensible search for further γ -ray source candidates may

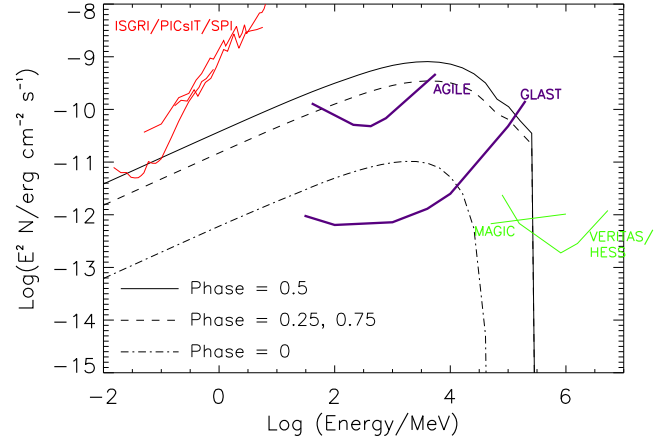


Fig. 5 IC spectra of WR 147 for orbital phases 0, 0.25, 0.5 and 0.75. See text for parameters. $\gamma\gamma$ pair production absorbs not more than $\leq 0.3\%$ (> 50 GeV) and $\leq 18\%$ (> 100 GeV) of the produced flux at orbital phases 0.25 and 0.5, respectively (not shown in figure). No absorption takes place at phase 0.

therefore start with scanning the WR-binary population for physically similar systems. A (not complete) list encompasses WR 146, WR 137, WR 112 and WR 125, with WR 112 being the most distant (~ 4 kpc) of them. From all of them non-thermal radio components have been observed at least occasionally. One (WR 137) has been found positionally coincident with an unidentified EGRET source (3EG J2016+3657: [9]).

5 Perspectives for the gamma-ray band

The identification of a specific colliding wind system or the population thereof as γ -ray emitters requires first: a convincing positional association, and second: its physical relation with the detected γ -ray source.

The most up-to-date catalog of WR-stars in the Milky Way lists more than 220 sources with a detected binary frequency of $\sim 40 - 50\%$ in the solar neighborhood [33]. Its spatial distribution reflects the spiral arm structure of our Galaxy with a slight asymmetry with respect to the galactic plane ([33] and references therein). 64 WR-(systems) are found in the solar neighbourhood (< 2 kpc), more than 25 have been detected in the immediate vicinity (< 30 pc) of the galactic center. The total number of WR-(systems) in the Galaxy has been estimated to up to ~ 8000 [34], total OB-star number counts in our Galaxy may reach values as high as 60000 [35]. This is orders of magnitude larger than the number of all, presumably galactic, but still unidentified γ -ray sources detected to date.

Intriguing positional coincidences of massive star populations, among them colliding wind systems, with unidentified EGRET sources have been found in the past (e.g.

[9,10]), however no individual binary system could unambiguously be identified as a high energy γ -ray emitter so far. This is most likely a statistical issue. EGRET's large location error box, typically $\sim 0.25^\circ$ for a strong point source at high latitudes, and even larger for sources in the galactic plane, allows to find many plausible counterparts within the positional uncertainty of the γ -ray source. Furthermore, the strong diffuse γ -ray background at low galactic latitudes makes the detection of any non-periodic galactic source close to the instrument sensitivity even more challenging. The capabilities of EGRET's successor, GLAST-LAT¹, will improve here. Its expected ability of both detecting weak signals ($> 3 \cdot 10^{-9} \text{cm}^{-2} \text{s}^{-1}$) and at the same time locating an object in the γ -ray sky within $\sim 0.5^\circ - 5'$, solves the confusion problem at least among the galactic bright EGRET sources.

How will a typical CWS appear at γ -ray energies? What are its observable characteristics that may discriminate it from the wealth of other plausible γ -ray source classes?

To begin with, the available energy kinetic wind energy $L_w = \dot{M}v_\infty^2/2$ provides a firm upper limit on the photon production rate from each process, and thus on the expected flux level. Inserting typical mass loss and wind parameters one finds the kinetic energy of massive star winds to be of order 1% of the bolometric radiative energy output, or typically $\sim 10^{38} \text{erg/s}$. Taking into account the efficiency of the particle acceleration process, much smaller values will rather be the rule.

Furthermore, colliding wind regions will appear not extended, but point-like on the γ -ray sky for both present and near future satellite and ground based instruments.

Our study implies that detectable phase-locked orbital variations in the γ -ray band occur, however, they may possibly be blurred by the geometry of the system (in particular due to eccentricity and inclination). Flux variations at high energies may additionally be expected from modulations of the geometry and size of the emitting region, modulations of the stellar target photon field density, inhomogeneities and/or shocks in the wind outflow, etc. The time scale of these variations is determined by the respective physical cause.

Spectral hints on the expected *low-energy* IC component of CWBs may be deduced from their visible synchrotron spectrum. Spectral indices at GHz frequencies in the range $\alpha_r=0.3\dots 1.3$ has been detected so far from the current limited sample of non-thermal emitters among the WR-binary systems. This may hint towards photon spectra with photon index $\alpha_{\text{ph}} < 2.5$ far below the cutoff energy. At GeV-energies KN, anisotropy and propagation effects may have an impact on the spectral shape.

With these characteristics at hand, a population study may be instrumental to finally unveil the class of massive star binary systems as high energy emitters.

Acknowledgements We like to thank the organizers of the conference "The multi-messenger approach to high energy gamma-ray sources", where this article was presented, for a very fruitful meeting.

References

1. Abbott, D.C., Biegging, J.H., Churchwell, E. & Torres, A.V. 1986, ApJ, **303**, 239 (1986)
2. Wright, A.E. & Barlow, M.J., MNRAS, **170**, 41 (1975)
3. White, R.L., ApJ, **289**, 698 (1985)
4. Völk, H.J. & Forman, M., ApJ, **253**, 188 (1982)
5. Chen, W. & White, R.L., ApJ, **366**, 512 (1991)
6. Pollock, A.M.T., A&A, **171**, 135 (1987)
7. White, R.L. & Chen, W., ApJ, **387**, 81 (1992)
8. Torres, D.F., Domingo-Santamaría, E., Romero, G.E., ApJ, **601**, L75 (2004)
9. Romero, G.E., Benaglia, P., Torres, D.F., A&A, **348**, 868 (1999)
10. Benaglia, P., Romero, G.E., Stevens, I.R. & Torres, D.F., A&A, **366**, 605 (2001)
11. Benaglia, P., Romero, G.E., Koribalski, B. & Pollock, A.M.T., A&A, **440**, 743 (2005)
12. Dougherty, S.M. & Williams, P.M., MNRAS**319**, 1005 (2000)
13. Leitherer, C., Chapman, J.M., Koribalski, B., ApJ, **450**, 289 (1995)
14. Leitherer, C., Chapman, J.M., Koribalski, B., ApJ, **481**, 898 (1997)
15. Williams P.M., van der Hucht, K.A., Pollock, A.M.T., et al., MNRAS, **243**, 662 (1990)
16. Chlebowski, T. & Garmany, C., ApJ, **368**, 241 (1991)
17. Pittard, J.M., Stevens, I.R., Williams, P.M. et al., A&A, **388**, 335 (2002)
18. Usov, V.V., ApJ, **389**, 635 (1992)
19. Eichler, D. & Usov, V., ApJ, **402**, 271 (1993)
20. Benaglia, P. & Romero, G.E., A&A, **399**, 1121 (2003)
21. Rauw, G., in "Cosmic Gamma-Ray Sources", Astrophysics & Space Science Library, Vol. **304**, Eds. Cheng K.S., Romero, G. (2004)
22. Mücke, A. & Pohl, M., in: "Interacting winds from massive stars", ASP conf. series, **260**, 355 (2002)
23. Gayley, K.G., Owocki, S.P. & Cranmer S.R., ApJ, **475**, 786 (1997)
24. Stevens, I.R. & Pollock, A.M.T., MNRAS, **269**, 226 (1994)
25. Mathys, G. in: "Variable and Non-spherical Stellar Winds in Luminous Hot Stars", eds. Wolf, B. et al., Lecture Notes in Physics, **523**, 95 (1999)
26. Iğance, R., Cassinelli, J.P. & Bjorkman, J.E., ApJ, **505**, 910 (1998)
27. Weber, E.J. & Davis, L.Jr., ApJ, **148**, 217 (1967)
28. Reimer, A., Pohl, M. & Reimer, O., A&A, **644**, 1118 (2006)
29. Reynolds, A.P., ApJ, **256**, 13 & 38 (1982)
30. Dougherty, S.M., Beasley, A.J., Claussen, M.J., et al., ApJ, **623**, 447 (2005)
31. Pittard, J.M. & Dougherty, S.M., MNRAS, in press (2006)
32. Setia Gunawan, D.Y.A., de Bruyn, A.G., van der Hucht, K.A., et al., A&A, **368**, 484 (2001)
33. van der Hucht, K.A., New Astronomy Reviews, **45**, 135 (2001) & van der Hucht, K.A., A&A Research Note, in press (2006)
34. Prantzos, N. & Casse, M., ApJ, **307**, 324 (1986)
35. Reed, B.C., AJ, **120**, 314 (2000)

¹ http://www-glast.slac.stanford.edu/software/IS/glast_lat_performance.htm